

## Estimation of intimate contact of the fusion-bonded fiber reinforced thermoplastic composites

ZHOU Jiakuan<sup>1,a\*</sup>, DESPLENTERE Frederik<sup>2,b</sup> and IVENS Jan<sup>1,c</sup>

<sup>1</sup>KU Leuven, Department of Materials Engineering, Campus De Nayer, Jan Pieter de Nayerlaan 5, 2860 Sint-Katelijne-Waver, Belgium

<sup>2</sup>KU Leuven, Department of Materials Engineering, Campus Bruges, Spoorwegstraat 12, 8200 Bruges, Belgium

<sup>a</sup>jiakuan.zhou@kuleuven.be, <sup>b</sup>frederik.desplentere@kuleuven.be, <sup>c</sup>jan.ivals@kuleuven.be

**Keywords:** Intimate Contact, Fusion Bonding, Fiber Reinforced Thermoplastic Composites, Surface Roughness, Viscosity

**Abstract.** The quality of fusion-bonded parts relies on the development of intimate contact at first and followed by healing, where the former as a prerequisite highly dominates the consolidation and the mechanical performance of final parts. In this paper, the degree of intimate contact of continuously welded unidirectional glass fiber reinforced polypropylene tapes was investigated. Classic Lee & Springer model for theoretical estimation of intimate contact was considered in the present study. For this purpose, a relatively robust regime to extract the data inputs like surface parameters, viscosity, etc. was proposed and demonstrated clearly. Consequently, the degree of intimate contact can be plotted as a function of time. Furthermore, the degree of intimate contact was also characterized by cross-sectional microscopy, ultrasonic C-scan, and optical analysis on the delaminated surfaces. The experimentally measured results show good agreement with the theoretically predicted counterparts.

### Introduction

Fiber reinforced thermoplastic composites (FRTPCs) have attracted more and more attention, as well as increasing applications in numerous industries, like automotive, aerospace and aeronautics. This is attributed to their nature of being lightweight but high-performance on the one hand, and more importantly, the flexibility and high efficiency in processing. With the thermoplastic matrix, FRTPCs are capable of being heated and solidified repeatedly, without losing mechanical performance itself. This enables FRTPCs to be recycled easily and eco-friendly, and be welded as well as repaired over and over. On this basis, lots of fusion-bonding-based processing techniques have been developed. However, the performance and quality of the fusion bonded parts at the end, heavily rely on the consolidation process.

The consolidation in the processing of FRTPCs, is attained by intimate contact between two substrates (can be tapes, prepregs, parts, etc.) at first, to eliminate asperities and voids at the interface. Afterward, the healing of the polymer-polymer interface can be achieved through interdiffusion and entanglement of polymer chains, driven by Brownian motion[1]. Importantly, the healing starts only at the interface where the intimate contact has been developed, and it cannot be activated if the intimate contact is not built. Therefore, intimate contact is a prerequisite of the following healing process, and also a foundation of the consolidation as well as bond strength building. This fact makes it highly dominates the integrity, durability and mechanical performance of final parts. In order to achieve good intimate contact, heating is necessary to soften and melt the polymer matrix, and pressure should also be applied to deform the asperities of FRTPCs by plastic deformation, squeeze flow and percolation flow. However, difficulties always exist. The resin-rich surface layer is always thought to be a merit for fusion bonding, but this is not always the case.

And, therefore, the polymer flow in the resin-poor regions is insufficient, making effective intimate contact challenging[2]. Moreover, thermoplastic polymers normally have a high viscosity, which means lower flowability and thus takes more time to spread and fill the interface. It wouldn't affect too much for techniques like autoclave molding or compression molding which has enough holding time, but more concern goes to fast processing techniques like automated fiber/tape placement, overextrusion, continuous welding (with hot gas torch), etc., which should achieve consolidation for a short duration, even within milliseconds[3].

Given the challenges in the achievement of intimate contact, a robust prediction model on the degree of intimate contact, as well as the regime for obtaining reliable data input should be well established. The essence of intimate contact processing makes it a function of temperature, pressure, and time. Furthermore, the nature of intimate contact development indicates that it is highly influenced by surface roughness, as well as the rheological behavior of melts. On this basis, there are already several different models for the estimation of degree of intimate contact, among which the Lee and Springer model[4], and the Yang and Pitchumani model[5, 6] are the most intensively used ones. Lee and Springer introduced the term "degree of intimate contact" for the first time, and their model follows the homogenizing ideology, by assuming a series of identical rectangles to represent the rough surface. Yang and Pitchumani model is more sophisticated, by describing the surface roughness as a Cantor set fractal morphology, which has a series of asperity generation with decreasing height. However, such a model is established with the assumption that the tape surface roughness behaviors fractal morphology, which is not always the case and limits the application of the Yang and Pitchumani model[7]. Moreover, it should be pointed out that intimate contact development is significantly influenced by the data inputs. Therefore, the acquisition of crucial parameters - surface parameters and viscosity, is decisive while has always been non-consensual and controversial. From the literature, there are prominent divergences in the model parameters, as well as the viscosity value to be used[8].

In summary, a robust model of intimate contact development is important, which is beneficial to the processing parameter optimization, and can be further used for the bond strength estimation. Therefore, in the present paper, we will contribute to a deeper understanding of intimate contact development and consolidation process, by investigating the degree of intimate contact ( $D_{ic}$ ) mathematically and experimentally, and by proposing more universal and robust criteria for the acquisition of modeling data inputs. To do so, non-isothermal in-situ consolidation, more specifically the continuous welding in the present study, was performed on unidirectional (UD) FRTPC tapes; Characterization on the used tapes was done to obtain the modeling data inputs; And the continuously welded FRTPCs were also inspected to reckon the  $D_{ic}$  for model validation. The attention is paid to the determination of mathematical model and corresponding parameters at first, based on the nature of used materials and the real processing conditions. Secondly, experimental works for the acquisition of data inputs were completed and discussed, giving the authors' opinions on the selection of experimental programs, and post-processing of the raw data. In particular, we will emphasize a solution to obtain surface parameters that are representative enough, and the determination of the viscosity value according to specific material nature and processing technique. Finally, several experimental investigations on the  $D_{ic}$  were performed, and a convenient method - optical analysis on the delaminated surfaces, was proposed.

### **Material and consolidation**

The FRTPC used in the present study is a commercial UD glass fiber reinforced polypropylene (GF/PP) tape from FRT tapes, with 0.25 mm thickness and 25 mm width. The matrix is a polypropylene homopolymer and has a melting point of around 166 °C. The fiber volume fraction is around 45%. The tape cross-section, as shown in the  $\mu$ CT slice in Fig. 1, reveals a smooth surface quality and nice resin-rich surface layers. Normally, those are desired merits for decent consolidation.

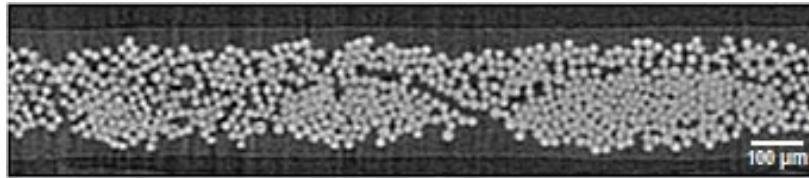


Fig. 1. A  $\mu$ CT slice of the raw GF/PP tape

The consolidation experiments were performed on a lab-scale continuous welding setup, as shown in Fig. 2. The setup is symmetrically assembled, consisting of two tape feedings, a heat source which is a hot gas torch in this study, a pair of stainless steel compaction roller which were set at a constant temperature of 5 °C (with the help of cooling units inside), and a pulling unit. This is the most fundamental unit for the manufacturing of 2-ply laminates, and it can be further assembled and upgraded for the manufacturing of multi-ply laminates.

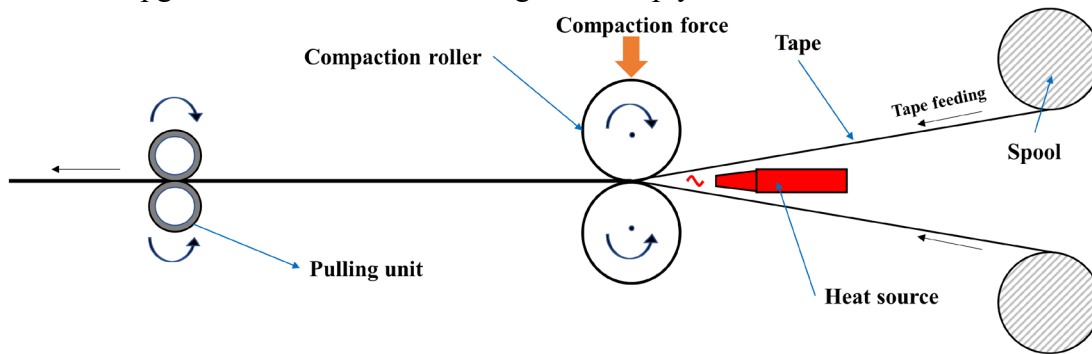


Fig. 2. A schematic of the continuous welding setup

For such kind of continuous welding process, a relatively high production speed is expected. For the sake of energy-saving and less impact on the internal structure of raw tape, an appropriate welding temperature is also desired together with line speed, to melt merely the resin-rich surface layer. Taking this into consideration, a series of 2-ply laminate consolidation experiments were done with the processing parameters given in Table 1. Please note that the set parameters may differ from the actual case, for example, the line speed in the table. The measurement of compaction pressure will be given in the corresponding section. As for the nip point temperature, there is a long-lasting difficulty in its measurement with the infrared camera. In this study, we will still treat what we measured as the nip point temperature, though it is not that but the tape inlet temperature. Furthermore, due to the hot gas torch in between the tapes and thus limited space for an infrared camera, we can only measure it from the side and give a rough temperature.

Table 1. Processing parameters for the continuous welding experiments

| Sample index | set line speed [m/min] | actual line speed [m/min] | set compaction pressure [MPa] | gas temperature [°C] | nip point temperature [°C] |
|--------------|------------------------|---------------------------|-------------------------------|----------------------|----------------------------|
| S1           | 3.5                    | 3.15                      | 0.1                           | 540                  | 190                        |
| S2           | 3.5                    | 3.15                      | 0.1                           | 580                  | 210                        |
| S3           | 3.5                    | 3.15                      | 0.1                           | 500                  | 175                        |
| S4           | 2.5                    | 2.19                      | 0.1                           | 540                  | 215                        |
| S5           | 2.5                    | 2.19                      | 0.1                           | 580                  | 235                        |
| S6           | 2.5                    | 2.19                      | 0.1                           | 500                  | 200                        |

### Mathematical model of intimate contact

Mathematical model. As mentioned before, basically all the existing models have been proven effective, once the corresponding assumptions meet with the actual material properties and processing conditions. In the present study, we use a smooth UD GF/PP tape as shown in Fig. 1. Such tape is supposed to be produced by extrusion/pultrusion, and therefore the surface roughness

should exhibit an extruded characteristic along the fiber direction, and the asperities are highly dependent on the spreading of the raw glass yarns. This possibly indicates that the surface roughness of GF/PP tape may not have a fractal nature. Taking this into consideration, and also for the sake of simplicity, the Lee and Springer model was used in this study.

Lee and Springer[4] treated the surface roughness as a succession of identical rectangles as shown in Fig. 3. The surface parameters are defined as identical rectangle height  $a_0$ , width  $b_0$ , and the gap width  $w_0$  initially. Moreover, a one-dimensional Newtonian flow was assumed, with the heat and compaction pressure applied. Consequently, the asperities, the rectangles in their model, can deform and flow, and get in contact with their counterparts gradually, as shown by the dashed rectangles in Fig. 3. Therefore, the  $D_{ic}$  was defined as the ratio between the surface area in physical contact and the projected tape surface area, and given as

$$D_{ic} = \frac{1}{1+\frac{w_0}{b_0}} \times \left[ 1 + \frac{5P_{app}}{\mu(T)} \left( 1 + \frac{w_0}{b_0} \right) \left( \frac{a_0}{b_0} \right)^2 t \right]^{\frac{1}{5}} \quad (1)$$

with related to time  $t$ , where  $P_{app}$  is the applied compaction pressure,  $\mu(T)$  is the temperature-dependent viscosity of the asperities/rectangles. A reliable description of surface roughness, asperity viscosity and compaction pressure is essential for a reasonable  $D_{ic}$  prediction.

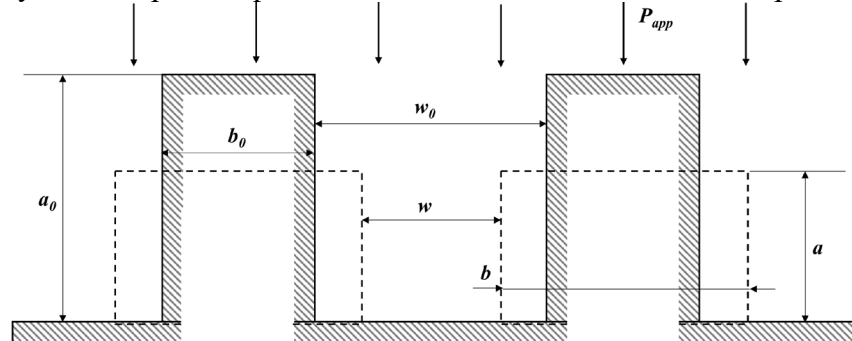


Fig. 3. A schematic of Lee and Springer's identical rectangle model

Surface parameter extraction. Surface parameters of the Lee and Springer model can be extracted from tape surface profiles, which are measured by a Sensofar S Neox 3D optical profiler in the present study. It is worth mentioning that in most literature the authors just gave their measurement with corresponding settings, and directly used it for surface parameter extraction. Moreover, it was also pointed out that the extraction of surface parameters can be tunable to fit with the experimental data[3]. Therefore, detailed procedures to do the measurements and post-processing should be clarified, and robust criteria should be established accordingly. A small-scale parametric study was done for this purpose (here due to the space limitation, we will not present too many details), giving the authors' remarks and suggestions at the end. The first important point, the raw data of the scanned profile always indicates the existence of form, resulting from the curved shape of the tape itself, or the unflattened posture. As shown in Fig. 4(a), the lower left is the lowest of the scanned surface while the upper right is the highest, due to the form (the warpage and mounting angle of the tape). To remove the form, a polynomial function can be applied, while it is key to select an appropriate order. We suggest trying different order values, and using the value that is capable of minimizing the difference between the maximum height and the arithmetical mean height of the surface profile. In this study, a polynomial function of order 12 was used, which revealed the extruded characteristic of asperities along the fiber direction, as can be seen from the striped pattern in Fig. 4(b). Moreover, the scanned area size should be large enough to ensure the representative of the extracted surface parameters. Meanwhile, a larger scanned area is normally stitched from multiple small scans, and this decreases the spatial resolution. To achieve balance between them, it is important to find the fundamental structure related to asperities. For the used GF/PP tape, the asperities exist in two spatial scales, first the

extruded ones and second the irregular micro hills on the extruded asperities. Thus the extruded asperities, normally around hundreds of microns, were regarded as the fundamental structure, and 5 to 10 times that scale should be determined as the dimension perpendicular to the fiber direction.

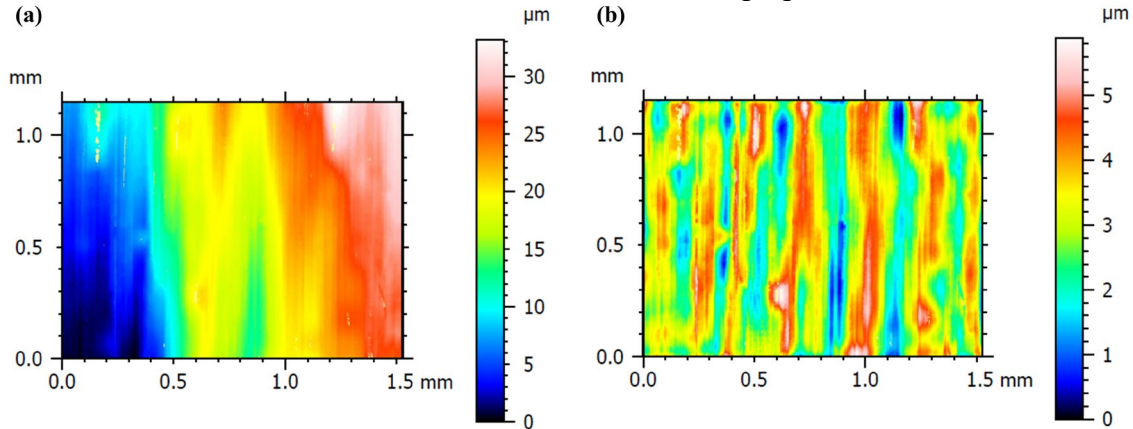


Fig. 4. (a) A pseudo-color view of the raw scanned surface; (b) After the form removal.

Following the remarks abovementioned, a 3D topography of GF/PP tape was obtained, and we started with extracting surface profiles that are perpendicular to the fiber direction, as the Lee and Springer model is a 2D squeeze flow model. A MATLAB script was developed to automatically extract the surface parameters, from the surface profiles. The script algorithm, see Fig. 5(a), follows similar steps from the literature[9], and several further modifications including the definition of the region of interest (ROI), width of asperities at the boundary, etc. Again, for the surface profile like Fig. 5(b), the surface parameter extraction is achieved by homogenizing the irregular asperities into identical rectangles with the same gap distance, like Fig. 5(c). It starts with doing interpolation but this is not mandatory, as this would benefit the accuracy more only when the asperities are extremely sharp. Second, the identical rectangle height  $a_0$  represents the mean height of all asperities, and therefore can be approximated as  $2\sigma$ , with  $\sigma$  the standard deviation of the surface profile. Third, the homogenization of irregular asperity width, should be done within a ROI, and it was defined as the whole region in between the highest and lowest profile point, across the whole length  $l$ . A series of horizontal reference lines (30 lines in this study) were assumed to be vertically distributed in the ROI with equal intervals. Thus, there were lots of intersections - the green dots in Fig. 5(b), which can be used to calculate each  $b_i$  as a corresponding asperity width at a specific vertical position. And the identical rectangle width  $b_0$  is the average of all  $b_i$  values. Lastly, as the area of the ROI, as well as that of asperities and of gaps should be equivalent before and after homogenization, we have

$$\frac{A_{gap}}{A_{asperity}} = \frac{ka_0w_0}{ka_0b_0} = \frac{w_0}{b_0} \quad (2)$$

with  $k$  the repeat numbers of identical rectangles. As the area of asperities and gaps can be calculated with numerical integration, the gap width  $w_0$  can be obtained. For the GF/PP tape, three surface profiles were analyzed and the corresponding surface parameters showed small deviation, thus the average of them was finally used, given as  $a_0 = 0.7693$ ,  $b_0 = 9.5965$ , and  $w_0 = 10.2441$ . These parameters also reflect the smooth nature of the GF/PP tape.

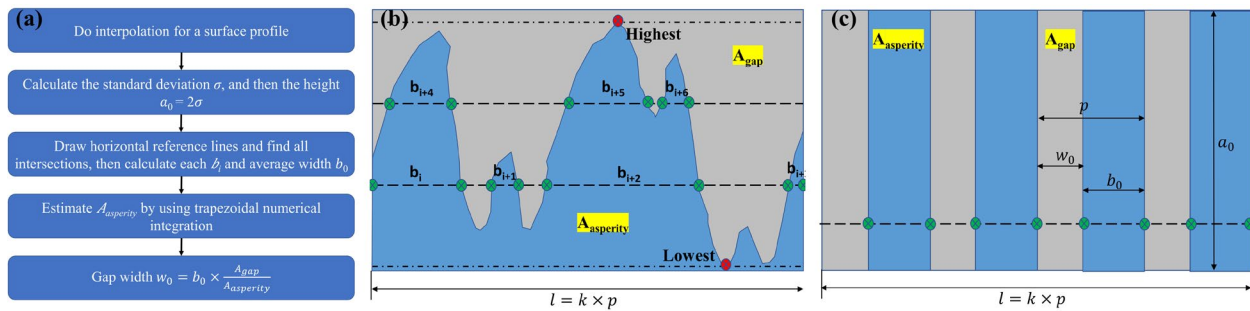


Fig. 5 Schematic of the surface parameter extraction

Viscosity measurement. The viscosity of the identical rectangles, or that of asperities, might be the most significant input parameter. On the one hand, due to the thermoplastic matrix, the viscosity is temperature-dependent. On the other hand, researchers [4], [9] were always struggling with which viscosity value to use, between that of neat polymer and that of fiber/matrix mixture. Moreover, it is worth mentioning that the viscosity values between them can vary by order of magnitude[10]. However, we would like to argue that the determination of viscosity value can be even more complex. The purpose of characterizing a viscosity is to depict the squeeze flow behavior of the contacting tape surfaces. Therefore, the key to determining what viscosity to use is actually to determine what is going to be squeezed flow, contributing to the intimate contact evolution. Some researchers [9], [11] considered the fact of resin-rich surface layer and smooth surface, and then used the viscosity of neat polymer. While once not the case, researchers tend to use the viscosity of fiber/matrix mixture, which is normally obtained based on squeeze flow theory, through compressing a FRTPC laminate[12]. Those assumptions may be reasonable. However, it is also typical that there is a resin-rich surface layer but also surface defects like dry fibers, making things a bit complex and thus introducing the definition of “effective intimate contact[2]”. Moreover, it is often overlooked that what is squeezed flow (or melted), can vary a lot under different processing and parameters, even for the same tape. An example is given by the GF/PP tape, as shown in Fig. 1, which has thick resin-rich surface layers (more or less than 2 times the fiber diameter) and smooth surfaces. If it is used for compression molding and thus being thoroughly melted in the thickness direction, then for sure the viscosity of its fiber/matrix mixture should be used for intimate contact modeling. However, if it is used for laser assisted tape placement with the laser being confined to merely melt the resin-rich surface layer, then the viscosity of neat polymer should be used. Moreover, though we are pursuing to melt merely the resin-rich surface layer, this cannot always be ensured considering different parameters and different heat sources. Under such circumstances, the melting depth in the tape thickness direction varies, and the viscosity of the melting part varies accordingly, between the viscosity of neat polymer and that of fiber/matrix mixture of whole tape thickness. This is extremely tricky and to the authors’ knowledge, there is no good method to characterize the corresponding viscosity for such a problem. Therefore, at least it is necessary to check the melting depth under specific conditions before decision.

For the continuous welding setup, and the processing parameters used in the present study, we managed to limit the heat input to melt merely the resin-rich surface layer. Fig. 6(a) shows a cross-sectional micrograph and from which we can see that the resin-rich surface layers were well maintained and there were no fibers being squeezed into the resin-rich surface layers. And Fig. 6(b) shows exterior photo of the as-manufactured 2-ply laminates, where the exterior surfaces of the laminates were not melt and as smooth as raw tape. Finally, we can determine that the viscosity of neat PP can be used in this study. It was measured using an Anton Paar plate-plate rheometer, with a plate diameter of 25 mm. Considering the temperature dependency, the viscosity was

measured from 180 °C to 240 °C, with a decreasing angular frequency  $\omega$  from 628 rad/s down to 0.1 rad/s. The as-measured data were fitted with the Carreau-Yasuda equation:

$$\eta^*(\omega) = \eta_\infty + (\eta_0 - \eta_\infty)(1 + (\lambda\omega)^a)^{(n-1)/a} \quad (3)$$

with the following parameters as given in Table. 2. The parameter  $\eta_0$  is the viscosity at zero shear rate, and it is suitable to represent the viscosity of the squeezed polymer in this study. Based on those values, the temperature-dependent viscosity can be fitted in the form of Arrhenius equation:

$$\mu(T) = (2.784E - 5) * e^{\frac{6.287E+4}{8.31T}} \quad (4)$$

with E the activation energy, R the universal gas constant, and T in Kelvin.

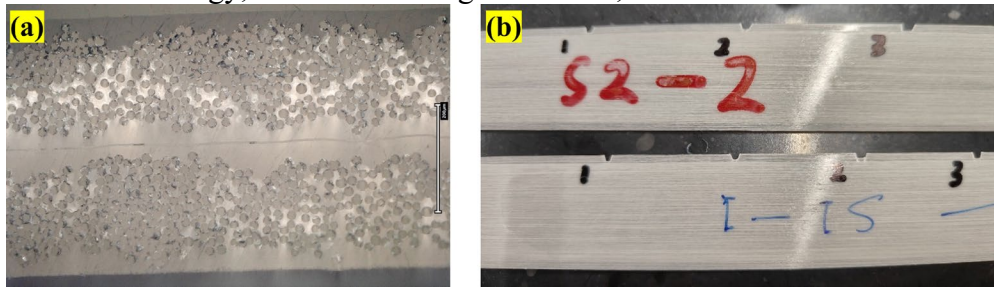


Fig. 6. (a) the micrograph and (b) exterior photo of the as-manufactured 2-ply laminates

Table 2. The fitted parameters for the complex viscosity of neat PP with the C-Y equation

| Temperature [°C] | $\eta_0$ [mPa.s] | $\eta_\infty$ [mPa.s] | $\lambda$ | $a$    | $n$    |
|------------------|------------------|-----------------------|-----------|--------|--------|
| 180              | 5.0451E+05       | 0.1000                | 0.0247    | 0.8032 | 0.4199 |
| 190              | 3.4846E+05       | 0.1000                | 0.0137    | 0.8034 | 0.3737 |
| 200              | 2.5713E+05       | 0.1000                | 0.0073    | 0.7481 | 0.2831 |
| 210              | 1.8655E+05       | 0.1000                | 0.0034    | 0.7607 | 0.0483 |
| 220              | 1.2484E+05       | 0.1000                | 0.0037    | 0.8684 | 0.1710 |
| 230              | 9.0521E+04       | 0.1000                | 0.0022    | 0.8516 | 0.0001 |
| 240              | 5.9637E+04       | 0.1000                | 0.0026    | 1.0445 | 0.0001 |

Compaction pressure measurement. Though the welding process is dynamic, we still measured the static pressure at room temperature instead. This is enough as the roller rotatory dynamic and the effect of molten matrix can be negligible for intimate contact development, and most researchers also made such an assumption for simplicity[2]. A piece of Fuji 4LW pressure measurement film was put on a tape, and between the compaction together. The measurement results, as shown in Fig. 7, reflect that the compaction area was small while asymmetric. The pressure distribution was more uniform than expected, indicating less edge effect. Thus, the compaction pressure was simplified into a uniform distribution of 0.107 MPa in a rectangle region of 3 mm width.

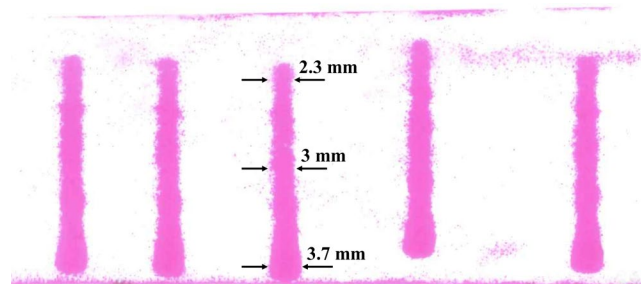


Fig. 7. The stained pattern on the pressure measurement film

Modeling results. Now that we obtained all the desired data inputs, the  $D_{ic}$  can be plotted with related to time, as shown in Fig. 8. Of course, the higher the temperature, the shorter the time to

achieve full  $D_{ic}$ , due to the temperature-dependent viscosity. Even at 180 °C, just a bit higher than the melting point, a full intimate contact can be achieved within around 2.6 s. Furthermore, the compaction time of samples given in Table 1 can be estimated with the corresponding actual line speed and the width of compaction region, which is around 0.0571 s for samples S1, S2 and S3, while 0.0822 s for samples S4, S5 and S6. On this basis, the corresponding  $D_{ic}$  can be calculated, as given in Table 3.

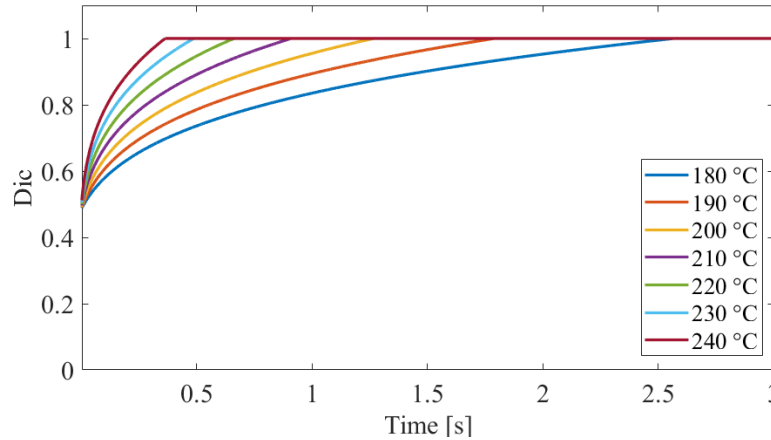


Fig. 8. The degree of intimate contact for the continuously welded GF/PP tape

Table 3. The degree of intimate contact for all the samples in this study

| Sample index | S1    | S2    | S3    | S4    | S5    | S6    |
|--------------|-------|-------|-------|-------|-------|-------|
| $D_{ic}$ [%] | 56.49 | 61.44 | 53.65 | 66.47 | 73.63 | 61.73 |

### Experimental inspection of intimate contact

Accurate and efficient experimental inspection of intimate contact is sometimes challenging. Cross-sectional microscopy[13] may be a solution, but it mainly provides 1D info at the interface and normally it is labor-intensive. X-ray computed tomography[9] proved its capability, but unfortunately, the poor image contrast between entrapped air and PP (also some other light polymers) limits its application in some glass fiber reinforced composites[14]. The authors also used ultrasonic C-scan, for example, a C-scan image of sample S4 in Fig. 9(a) and its thresholding (with white denoting the non-contacting region) in Fig. 9(b), which resulted in an average  $D_{ic} = 52.66\%$ . According to the comparison with its cross-sectional microscopy, it turned out that, the thresholding and thus the  $D_{ic}$  is not good due to fibers and matrix’s anisotropy in such a thin laminate. Moreover, the distribution of non-contact regions is quite uneven, in a relatively large area. This indicates that the method of inspecting the intimate contact in a large area should be more representative, and necessary.



Fig. 9. (a) the C-scan image and (b) its thresholding result of a S4 sample

Afterward, the authors proposed to inspect the intimate contact by optical analysis on the delaminated surfaces. This was done by guiding the two tape feeding separately over a second roller right behind the compaction roller, this way the welded tapes can be immediately delaminated. Considering that the relaxation time of PP, which is the  $\lambda$  in Table 2, is really small, we assume that all regions that achieve intimate contact should also start or even finish the autohealing, and thus there should be polymer chains across the interface in those regions. Therefore, once the tape is delaminated, those intimate contact regions should suffer from damage, normally plastic deformation and stress whitening. As can be seen from Fig. 10(a), there are milky opaque regions like the one denoted by a red dot, assumed to be intimate contact regions in this study. While the relatively translucent regions like the one denoted by a green dot are non-contacting. Following this idea, a better direct thresholding was obtained as shown in Fig. 10(b), and gave the  $D_{ic} = 66.8\%$ . This method inspects the intimate contact development of a large area in an efficient manner, giving a decent  $D_{ic}$ . However, it is worth mentioning that the delaminated surface image of weakly bonded samples may not have enough contrast, and therefore it is necessary to manually enhance the contrast at first.



Fig. 10. (a) an image of the delaminated surface and (b) its thresholding result of a S4 sample

## Conclusion

In this study, we used the Lee and Springer model to estimate the  $D_{ic}$  of continuously welded GF/PP, and proposed a method of optical analysis on the delaminated surfaces to investigate the  $D_{ic}$ , which gave a decent result and agreed well with the modeling result. More importantly, the authors contribute to the fulfillment of reliable data input extraction for mathematical modeling. Relatively robust criteria to process the scanned 3D surface topography were obtained through a small-scale parametric study, and the surface parameters can be automatically extracted from real 3D surfaces with the developed MATLAB script. This ensures the acquired surface parameters are solid and reliable. Moreover, the authors demonstrate the keys to determining the asperity viscosity to use, emphasizing that the melting depth of the tape in the thickness direction should also be taken into consideration, which highly depends on both the nature of the tape and the processing techniques as well as parameters.

## References

- [1] I. Martin, D. Saenz Del Castillo, A. Fernandez, and A. Güemes, Advanced thermoplastic composite manufacturing by in-situ consolidation: A review, *J. Compos. Sci.*, 4 (2020) 1–36. <https://doi.org/10.3390/jcs4040149>
- [2] O. Çelik, D. Peeters, C. Dransfeld, and J. Teuwen, Intimate contact development during laser assisted fiber placement: Microstructure and effect of process parameters, *Compos. Part A Appl. Sci. Manuf.*, 134 (2020) 105888. <https://doi.org/10.1016/j.compositesa.2020.105888>
- [3] M. J. Donough, Shafaq, N. A. St John, A. W. Philips, and B. Gangadhara Prusty, Process Modelling of In-situ Consolidated Thermoplastic Composite by Automated Fibre Placement – A Review, *Compos. Part A Appl. Sci. Manuf.*, (Dec. 2022) 107179. <https://doi.org/10.1016/J.COMPOSITESA.2022.107179>

- [4] W. Il Lee and G. S. Springer, A Model of the Manufacturing Process of Thermoplastic Matrix Composites, *J. Compos. Mater.*, 21 (1987) 1017–1055. <https://doi.org/10.1177/002199838702101103>
- [5] F. Yang and R. Pitchumani, A fractal Cantor set based description of interlaminar contact evolution during thermoplastic composites processing, *J. Mater. Sci.*, 36 (2001) 4661–4671. <https://doi.org/10.1023/A:1017950215945>
- [6] F. Yang and R. Pitchumani, Fractal description of interlaminar contact development during thermoplastic composites processing, *J. Reinf. Plast. Compos.*, 20 (2001) 536–546.
- [7] A. Levy, D. Heider, J. Tierney, and J. W. Gillespie, Inter-layer thermal contact resistance evolution with the degree of intimate contact in the processing of thermoplastic composite laminates, *J. Compos. Mater.*, 48 (2014) 491–503.
- [8] M. A. Khan, P. Mitschang, and R. Schledjewski, Identification of some optimal parameters to achieve higher laminate quality through tape placement process, *Adv. Polym. Technol.*, 29 (Jun. 2010) 98–111. <https://doi.org/https://doi.org/10.1002/adv.20177>
- [9] P. M. Schaefer, T. Guglhoer, M. G. R. Sause, and K. Drechsler, Development of intimate contact during processing of carbon fiber reinforced Polyamide-6 tapes, *J. Reinf. Plast. Compos.*, 36 (2017) 593–607. <https://doi.org/10.1177/0731684416687041>
- [10] P. M. Schäfer, Consolidation of carbon fiber reinforced polyamide 6 tapes using laser-assisted tape placement. Technische Universität München, 2017.
- [11] W. J. B. Grouve, L. L. Warnet, B. Rietman, H. A. Visser, and R. Akkerman, Optimization of the tape placement process parameters for carbon-PPS composites, *Compos. Part A Appl. Sci. Manuf.*, 50 (2013) 44–53. <https://doi.org/10.1016/j.compositesa.2013.03.003>
- [12] J. Engmann, C. Servais, and A. S. Burbidge, Squeeze flow theory and applications to rheometry: A review, *J. Nonnewton. Fluid Mech.*, 132 (2005) 1–27.
- [13] O. Çelik *et al.*, The influence of inter-laminar thermal contact resistance on the cooling of material during laser assisted fiber placement, *Compos. Part A Appl. Sci. Manuf.*, 145 (2021) 106367.
- [14] J. Zhou, F. Desplentere, and J. Ivens,  $\mu$ CT-based internal microstructure analysis in continuous fiber reinforced thermoplastics, in *ITHEC 2022 Conference Proceedings*, CONGRESS BREMEN & MESSE BREMEN, 2022.